PHYSICAL REVIEW B VOLUME 27, NUMBER 4 15 FEBRUARY 1983

Deformation parameter and ultrasonic attenuation in the nearly-free-electron model

Harjeet Kaur and Sushil Auluck
Physics Department, University of Roorkee, Roorkee-247672, India
(Received 25 May 1982)

We present a model calculation of the effect of Fermi-surface distortions introduced by a pair of Bragg planes on the deformation parameter and the ultrasonic attenuation.

I. INTRODUCTION

In the past few years there have not been very many attempts to understand the behavior of the ultrasonic attenuation in metals. In calculating the ultrasonic attenuation we have to first determine the deformation potential. Unfortunately, this quantity has not attracted much attention. Almost all calculations of the ultrasonic attenuation use the free-electron deformation potential given first by Pippard.[1] Even some more recent calculations of the ultrasonic attenuation that employ detailed knowledge of the Fermi surface use the free-electron deformation potential or some simple modification of it.[2–5] In this paper we present a model calculation of the effect of the Fermi-surface distortions on the deformation potential and the ultrasonic attenuation. For our work we use the nearly-free-electron model where the Fermi-surface distortions are introduced by a pair of Bragg planes.

We report here model calculations of the deformation potential and ultrasonic attenuation for a sound wave propagating perpendicular to the Bragg planes (c axis). We feel that for sound waves along this direction there should be the maximum deviation from the free-electron case because in this direction the effective zones are perturbed significantly. For sound waves perpendicular to this we expect the least deviation from the free-electron case. Thus our results, when compared with the free-electron case, would give an idea about the anisotropy of the deformation potential and ultrasonic attenuation.

The plan of the paper is as follows. In Sec. II we give a calculation of the deformation potential using the nearly-free-electron model for the Fermi surface. In Sec. III we calculate the ultrasonic attenuation using the free-electron deformation potential and a distorted Fermi surface. In Sec. IV we give the results of the ultrasonic attenuation using the nearly-free-electron deformation potential on the one hand and a distorted Fermi surface on the other. Our conclusions are summarized in Sec. V.

II. CALCULATION OF THE DEFORMATION POTENTIAL

In calculating the ultrasonic attenuation it is the deformation potential D which is the fundamental parameter in the theory. The deformation potential D is given by[1,2]

$$D = K_x + k_x \cos\phi \ , \tag{1}$$

where k_x is the component of the electron wave vector along the propagation direction, ϕ is the angle between the propagation direction and the surface normal, and K_x is the deformation parameter for static longitudinal strain along the x axis such that for a strain w_x the Fermi surface (FS) at k will move normal to itself by $K_x w_x$. A detailed discussion of the properties of D have been given by Pippard.[1] In our case, while calculating the deformation potential, K_x is taken as isotropic but actually it depends on direction. The property of charge conservation requires that[1,2]

$$\int_{\mathrm{FS}} D \, ds = \int_{\mathrm{FS}} (K_x + k_x \cos\phi) ds = 0 \ , \tag{2}$$

where ds is the surface-area element. We do not have to calculate the deformation parameter on the Brillouin zone since $K_x + k_x \cos\phi$ is identically zero on a Brillouin zone.

For a metal with a spherical Fermi surface it is trivial to evaluate the integral of Eq. (2), and one obtains $K_x = -\frac{1}{3} k_F$. In the absence of any better calculation of K_x workers have used the free-electron K_x to determine the ultrasonic attenuation for metals with a complicated Fermi surface. In this paper we make the first attempt to obtain K_x beyond the free-electron approximation, i.e., in the nearly-free-electron approximation.

We calculate K_x for a Fermi surface which is

spherical in most of the region but distorted by a pair of parallel Bragg planes. With some modifications our model could be applied to the hexagonal close-packed metals. We take K_x to be independent of $\vec{k}$ in the first approximation but to depend on direction and, for reasons mentioned above, we take the propagation direction to be perpendicular to the Bragg planes. For the above-mentioned direction we obtain in the I region

$$K_xS=\pi(-G(G^4+4V^2)^{1/2}/8-2X^3/3+GX^2/2-V^2\{\ln[G^2+(G^4+4V^2)^{1/2}]\}/2G$$
$$-[(G^2-2XG)^2+4V^2]^{1/2}[(G-2X)/8-G/4]$$
$$+V^2\ln\{(G^2-2XG)+[(G^2-2XG)^2+4V^2]^{1/2}\}/2G), \quad E<\frac{G^2}{4}-V, \tag{3}$$

in the II region

$$K_xS=\pi\{G^3/24+GV/2+V^2\ln(2V)/2G-V^2\ln[G^2+(G^4+4V^2)^{1/2}]/2G$$
$$-G(G^4+4V^2)^{1/2}/8\}, \quad \frac{G^2}{4}-V<E<\frac{G^2}{4}+V, \tag{4}$$

and in the III region

$$K_xS=\pi(GY^2/2+GV+V^2\ln(2V)/G-V^2\ln[(G^4+4V^2)^{1/2}+G^2]/2G$$
$$-G(G^4+4V^2)^{1/2}/8-2Y^3/3+[(G-2Y)/8-G/4][(G^2-2YG)^2+4V^2]^{1/2}$$
$$-V^2\ln\{(G^2-2YG)+[(G^2-2YG)^2+4V^2]^{1/2}\}/2G), \quad E>\frac{G^2}{4}+V, \tag{5}$$

where

$$X=G/2-[E+G^2/4-(EG^2+V^2)^{1/2}]^{1/2} \tag{6}$$

and

$$Y=G/2+[E+G^2/4-(EG^2+V^2)^{1/2}]^{1/2}, \tag{7}$$

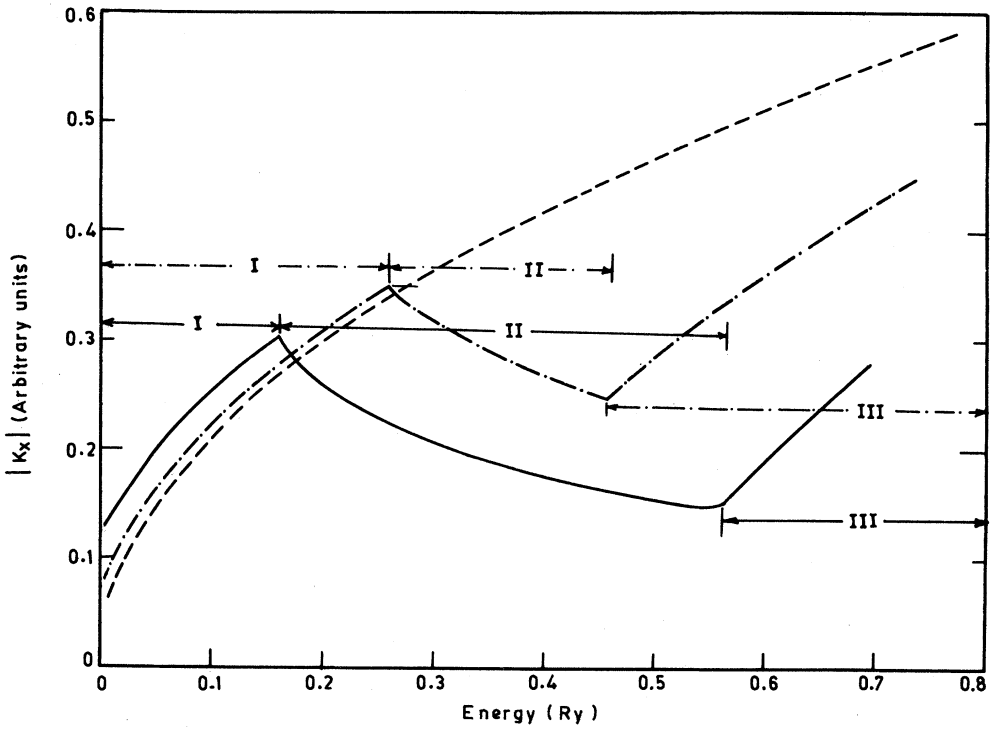

FIG. 1. Deformation parameter K_x as a function of energy for different values of V. --- for $V=0.0$ Ry, -·-·- for $V=0.1$ Ry, and — for $V=0.2$ Ry.

and where S is the surface area that has been calculated numerically, E is the energy (in Ry), G ($=1.2$ a.u., typical of the group-II*a*, -II*b*, hexagonal close-packed metals) is the reciprocal lattice corresponding to the Bragg planes of interest, and V is a pseudopotential parameter.

Our expressions for the deformation parameter reduces to the free-electron case in the I and III regions while evaluating with $V=0.0$. In the II region there is no energy dependence for K_x, and this is similar to the density of state $N(E)$ in this region. In Fig. 1 we plot $|K_x|$ as a function of energy for the free-electron case and for the nearly-free-electron case with two different potentials. For the free-electron case the curve varies as $(E)^{1/2}$, but as we include the potential we see a different behavior of the deformation parameter. We note the following: (i) All the three different energy regions have different Fermi-surface topologies and this manifests itself very clearly for K_x in Fig. 1; (ii) In the I and III regions of energy $|K_x|$ increases with energy, but in region II it decreases with energy. This is due to the fact that, as we see from the expression for K_x in this region, there is no energy dependence in K_x. For this region there is energy dependence only due to the surface area S, and the surface area increases with energy so $|K_x|$ decreases with energy; (iii) In the I region of energy we call this $K_{||}$, and the free electron (FE) K_x will not be much different from the $K_\perp$ for the wave propagating perpendicular to the c axis (taken perpendicular to the Bragg planes). So we take $K_{FE}=K_\perp$. Thus we see that K_x is larger than the free-electron value, i.e., $|K_{||}|>|K_\perp|$, but in the II and III regions $|K_\perp|>|K_{||}|$. We also note that $1-|K_{||}/K_\perp|$ depends on V and that in the II region the factor $1-|K_{||}/K_\perp|$ depends on energy more strongly than in the I and III regions.

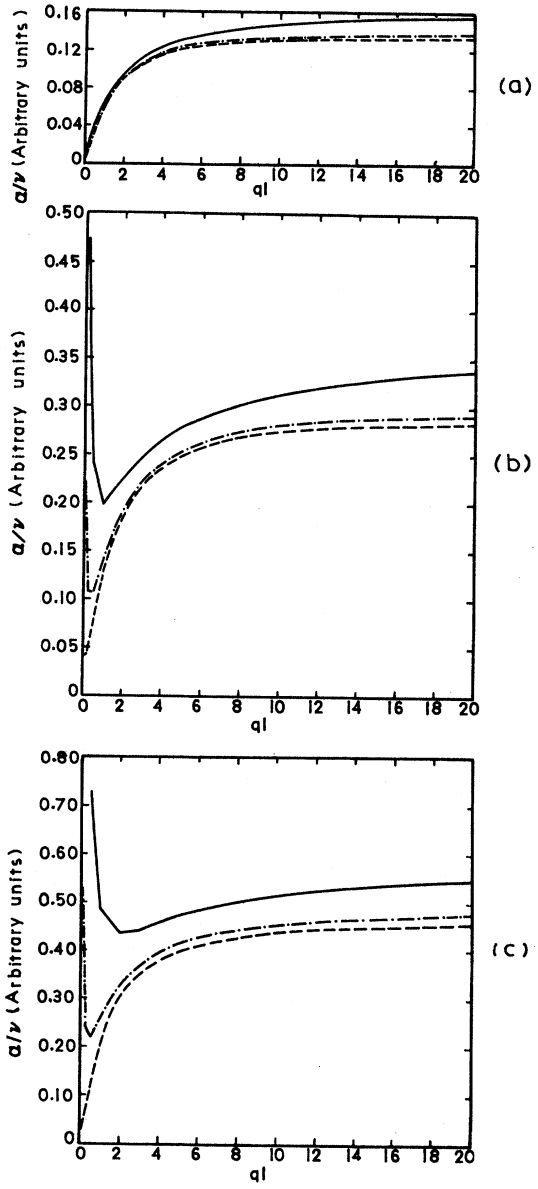

FIG. 2. α/ν (in units of $\hbar/2\pi^2Mv_s^2$) calculated with $K_x=-\frac{1}{3}k_F$ as a function of energy for three different values of V. --- for $V=0.0$ Ry, -·-·- for $V=0.05$ Ry, and — for $V=0.1$ Ry. (a) For $E<G^2/4-V$ (I region). (b) For $G^2/4-V<E<G^2/4+V$ (II region). (c) For $E>G^2/4+V$ (III region).

III. CALCULATION OF THE ULTRASONIC ATTENUATION

For a real metal with an arbitrary Fermi surface the electronic attenuation α of a longitudinal sound wave can be written as[1,2]

$$\alpha=\frac{\hbar q}{4\pi^3 M v_s}\left[\int\frac{D^2a\,ds}{1+a^2\cos^2\phi}+\frac{\left[\int D\,ds/(1+a^2\cos^2\phi)\right]^2}{\int(a\cos^2\phi)/(1+a^2\cos^2\phi)ds}\right]. \tag{8}$$

In this equation M is the density of the metal, v_s is the sound velocity, and a is the product ql, where q is the wave number of the ultrasonic wave, and l is the electron mean free path, which is assumed to be impurity limited and isotropic. The integral is over the Fermi surface. For a spherical Fermi surface

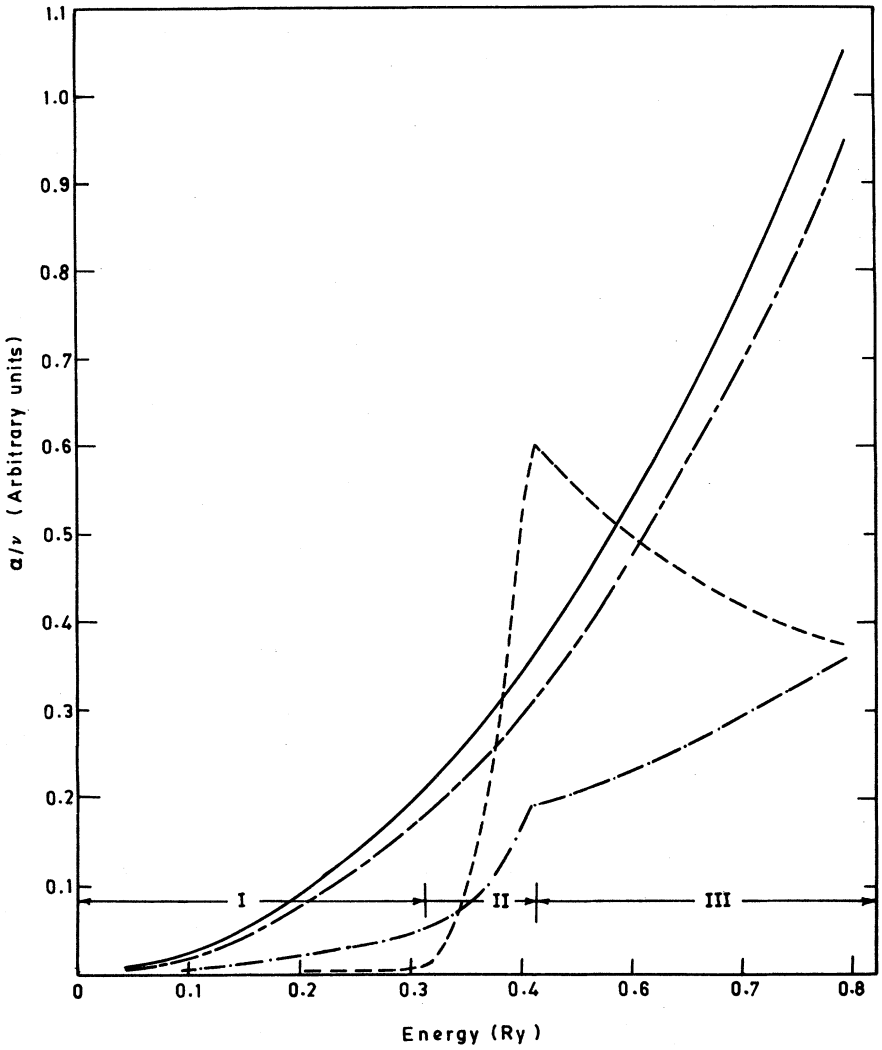

FIG. 3. α/ν (in units of $\hbar/2\pi^2 M v_s^2$) calculated with $K_x = -\frac{1}{3}k_F$ as a function of energy for potential $V=0.05$ Ry and for four different values of ql. --- for $ql=0.1$, -·-·- for $ql=0.5$, ——— for $ql=5.0$, and — for $ql=20.0$.

the above integrals can be solved analytically, but when the Fermi surface is distorted, the integrations have to be done numerically. To see the effect of Fermi-surface distortions on α, we have calculated α with $K_x = -\frac{1}{3}k_F$ and the Fermi surface as given by the nearly-free-electron model. It is customary to plot α/ν, where ν is the frequency of the sound wave, as a function of ql. This will change the prefactor of Eq. (8) to $\hbar/2\pi^2 M v_s^2$. In Fig. 2 we have plotted α/ν as a function of ql for the three different energy regions. The calculated α/ν is in units of $\hbar/2\pi^2 M v_s^2$. For each region we have plotted α/ν for $V=0.0$, 0.05, and 0.1 Ry. We note that the attenuation increases with increasing V. The trend for large ql remains the same as in the free-electron case. At small ql there seem to be marked deviations from free-electron behavior. Moreover, for small ql, α/ν decreases with increasing ql. This could perhaps be due to the fact that for small ql the whole Fermi surface contributes to α, and since K_x is constant, the distorted Fermi surface seems to be giving a significant contribution to α/ν. We feel that this trend in α/ν is an artifact of our model and seems to suggest the importance of calculating K_x correctly.

As described earlier in the Introduction, we can assess the anisotropy in α/ν by comparing our results with the free-electron case. We see that in all three regions $|\alpha_{||}/\alpha_{\perp}| > 1$ and, as we increase the potential, the anisotropy in α/ν is also increased.

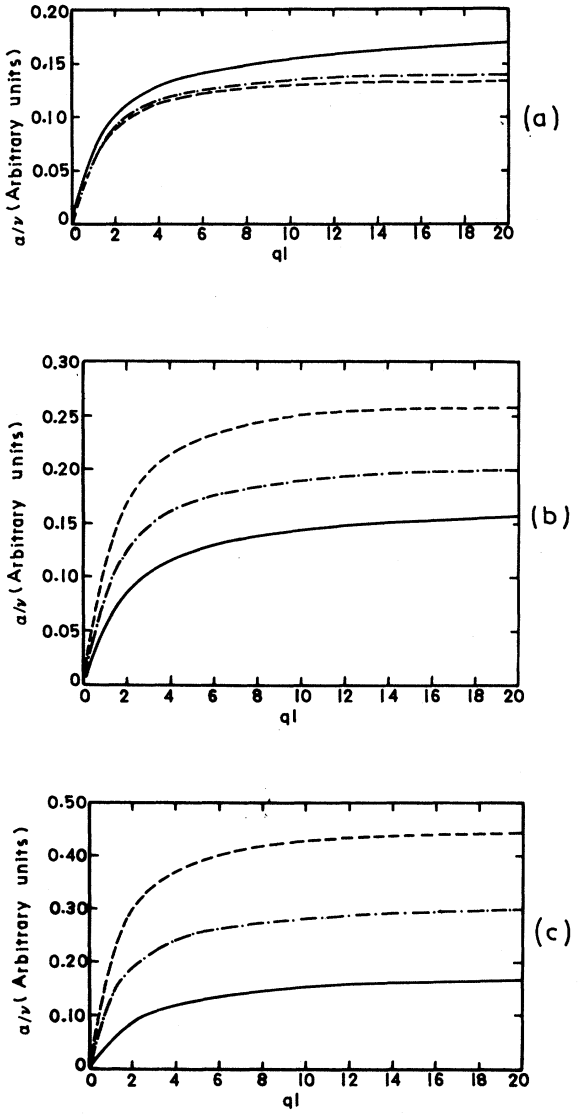

FIG. 4. Same as in Fig. 2 but with K_x calculated as given in the text.

In order to see the effect of Fermi-surface distortion we have plotted α/ν as a function of energy for various ql taking $V=0.05$ Ry in Fig. 3. For large ql the α/ν value is the same as in the free-electron case. For small ql, however, significant deviations from the free-electron behavior are seen. In fact, the effect of the Fermi-surface shape on α/ν is easily seen in this figure with sharp cusps at $E=G^2/4\pm V$. The rapid change in α/ν for $ql=0.1$ in the III region, and the not so rapid change in α/ν in III region, seem to indicate the unreliability of K_x.

IV. RESULTS

As mentioned in the preceding section, there seems to be some doubt in the correctness of α/ν when using the free-electron deformation potential and nearly-free-electron Fermi surfaces especially for small ql. We have, therefore, calculated α/ν using the deformation potential calculated in Sec. II and the nearly-free-electron Fermi surface. Our results are plotted in Fig. 4 for all three energy regions. We note that the strange behavior of small ql has disappeared. This reiterates our view that in order to calculate α/ν correctly for a deformed Fermi surface we need to calculate K_x for the deformed Fermi surface. We note in Fig. 4 that (i) In the I region the value of attenuation increases with potential energy, i.e., $|\alpha_{\parallel}| > |\alpha_{\perp}|$, so the anisotropy increases with potential energy. This behavior is a reflection of the K_x behavior; (ii) In the III$_1$ region of energy α/ν decreases with potential energy. This is because K_x decreases with energy in this region as shown in Fig. 1. Also, $|\alpha_{\parallel}/\alpha_{\perp}| < 1$ and the anisotropy of α/ν decreases with potential energy; (iii) In the III region too, the anisotropy of α/ν and K_x decreases with potential energy, as can be seen in Fig. 1.

In Fig. 5 we have plotted α/ν as a function of energy for various ql and $V=0.05$ Ry. We note that in the I and III regions of energy the trend of α/ν is similar to that of the free-electron case, but in the II region α/ν decreases slightly with energy. This trend of α/ν in the II region is due to K_x, which also decreases with energy in this region. We also see that the strange behavior of α/ν for small ql does not appear for this case.

V. CONCLUSIONS

We have given a model calculation of α/ν for a distorted Fermi surface, using the deformation parameter K_x calculated for a distorted Fermi surface. This contrasts with other workers who have calculated α/ν for a distorted Fermi surface but with the free-electron deformation parameter. Our results show that to obtain the correct behavior of α/ν for small ql, we have to calculate the deformation parameter K_x exactly. The geometrical features of the Fermi surface can be used to explain the anisotropy in the electronic ultrasonic attenuation. We have shown the following: (i) The anisotropy of the deformation parameter K_x and the ul-

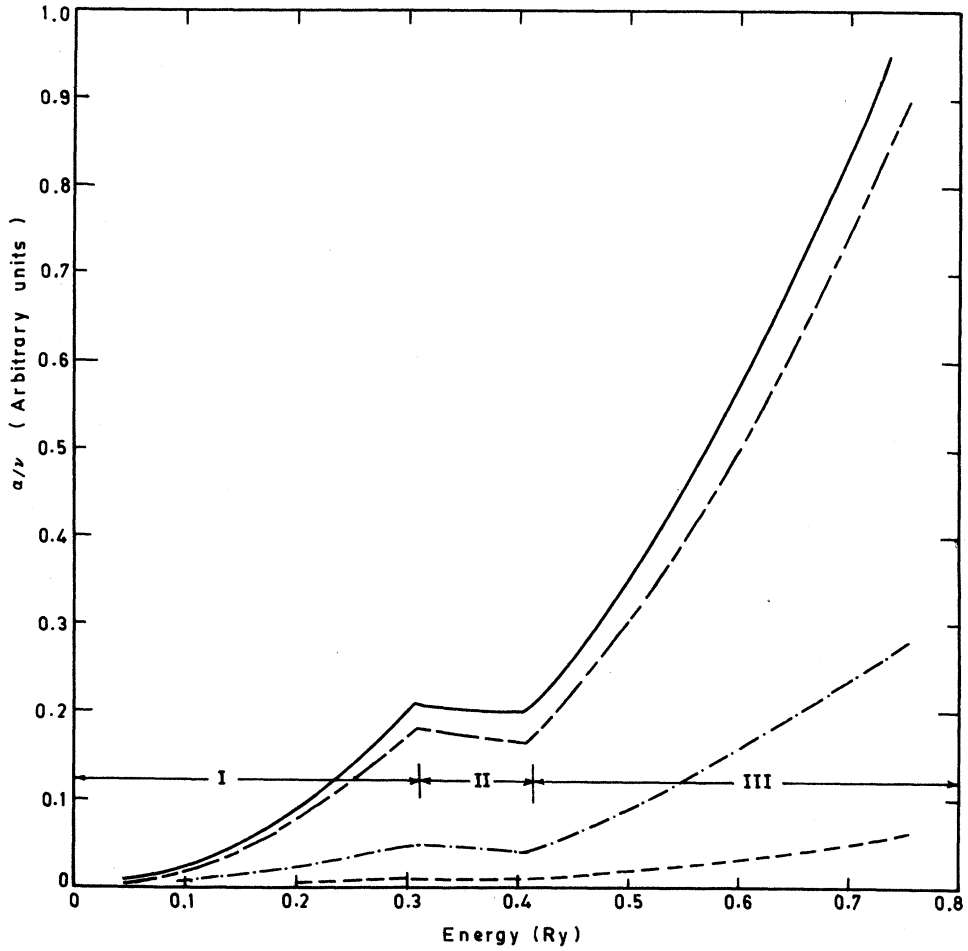

FIG. 5. Same as in Fig. 3 but with K_x calculated as given in the text.

trasonic attenuation α increases with potential energy for $E < G^2/4 + V$; (ii) In the region $G^2/4 - V < E < G^2/4 + V$ and $E > G^2/4 + V$ the anisotropy of the deformation parameter and the ultrasonic attenuation decreases with the potential energy.

ACKNOWLEDGMENTS

We would like to thank the Council of Scientific and Industrial Research (India) and the Dean of the Research and Industrial Liaison (Roorkee) for financial support.

[1]A. B. Pippard, Proc. R. Soc. London, Ser. A 257, 165 (1960).
[2]K. C. Hepfer and J. A. Rayne, Phys. Rev. B 4, 1050 (1971).
[3]B. Berre and A. Vetleseter, J. Low Temp. Phys. 7, 399 (1972).
[4]J. Trivisonno and R. W. Stark, J. Low Temp. Phys. 32, 725 (1978).
[5]M. J. Lea, J. D. Llewellyn, D. R. Peck, and E. R. Dobbs, Proc. R. Soc. London, Ser. A 334, 357 (1973).